$$g_{x'}^{av} = \tfrac{1}{2}\cos^2\epsilon[(g_{x'}\cos^2\eta + g_{y'}\sin^2\eta)(1+P) + g_{z'}(1-P)] + \sin^2\epsilon(g_{x'}\sin^2\eta + g_{y'}\cos^2\eta) - 2\sin\epsilon\cos\epsilon\sin\eta\cos\eta(g_{x'} - g_{y'})Q \quad (11a)$$

$$g_{y'}^{av} = \tfrac{1}{2}\sin^2\epsilon[(g_{x'}\cos^2\eta + g_{y'}\sin^2\eta)(1+P) + g_{z'}(1-P)] + \cos^2\epsilon(g_{x'}\sin^2\eta + g_{y'}\cos^2\eta) + 2\sin\epsilon\cos\epsilon\sin\eta\cos\eta(g_{x'} - g_{y'})Q \quad (11b)$$

$$g_{z'}^{av} = \tfrac{1}{2}[(g_{x'}\cos^2\eta + g_{y'}\sin^2\eta)(1-P) + g_{z'}(1+P)] \quad (11c)$$

the $\boldsymbol{g}$ principal values of the rigid low-temperature configuration. ϵ and η describe the angle between the principal axis of $g_{x'}$ and x'' and the direction of the axis of $g_{x'}^{av}$, respectively (see Figure 9d). $P = \sin\alpha\cos\alpha/\alpha$ and $Q = \sin\alpha/\alpha$, where α denotes the half-amplitude of the restricted oscillation. For $\eta = \epsilon = 0$, eq 11a-c reduce to the expressions given by Van et al.[58] Both types of motions, wobbling or oscillation of O_β, are not able to adequately describe the experimental data. Wobbling cannot explain the observed rotation of $g_{x'}$ and $g_{y'}$ by $\eta = 25°$ around $\overline{O_\alpha O_\beta}$. On the other hand, the small room-temperature value of $g_{z'}^{av} = 2.049$ leads to an unreasonably large angle α for the oscillation model. In addition, for a quantitative calculation of the disorder of O_β a distribution function had to be introduced.

The motion of O_β in $B_{12r}O_2$ will therefore qualitatively be best described as an oscillation in a plane inclined to ring C, which is superimposed by a certain amount of wobbling. This type of disorder of O_β is illustrated in Figure 9d. Such a motion of the dioxygen fragment explains both observations, the strong decrease of the largest diagonal element of $\mathbf{g}$ and the conservation of the traces of $\mathbf{g}$ and $\mathbf{A}^{Co}$ with increasing temperature. It also causes a considerable decrease of $A_{x'}^{17O}$. Similar disorder of the σ-bonded O_2 molecule in cobalt dioxygen adducts at ambient temperature have been observed in a number of X-ray investigations.[5,6,7,8,51] The different types of disorder models proposed in these studies are summarized in Table V.

Acknowledgment. We express our gratitude to Sandoz AG, Basle, for financial support. We also thank Prof. J. H. Ammeter for the opportunity to measure Q-band spectra on his spectrometer. Furthermore we are grateful to Dr. M. Rudin for helpful discussions, to W. Businger for technical assistance with the high-pressure experiments, to Dr. T. Dschen for his data processing program PACKAGE, and to C. Rey for the preparation of the single crystals.

Registry No. $B_{12r}O_2$, 12581-61-2.

(58) Van, S. P.; Birrell, G. B.; Griffith, O. H. *J. Magn. Reson.* **1974**, *15*, 444-459.
(59) Morton, J. R. *Chem. Rev.* **1964**, *64*, 453-471.

Mixed-Valence Chemistry of Adjacent Vanadium Centers in Heteropolytungstate Anions. 1. Synthesis and Electronic Structures of Mono-, Di-, and Trisubstituted Derivatives of α-$[P_2W_{18}O_{62}]^{6-}$ [1]

Subhash P. Harmalker, Michele A. Leparulo, and Michael T. Pope*

Contribution from the Department of Chemistry, Georgetown University, Washington, D.C. 20057. *Received November 29, 1982*

Abstract: Heteropolytungstates α-$[P_2(W,V)_{18}O_{62}]^{n-}$ containing respectively one (α_2-V), two (V_2), and three (V_3) vanadium atoms in one of the two equivalent M_3O_{13} "caps" of the α-$P_2W_{18}O_{62}$ structure have been synthesized and characterized by ^{31}P and ^{51}V NMR spectroscopy, electrochemistry, and optical and ESR spectroscopy of reduced and mixed-valence derivatives. The latter species show 15-line (V_2), 22-line (V_3), and 36-line (V_3) ESR spectra at 300-350 K, which collapse to "normal" eight-line spectra at <100 K. The complexes therefore are class II mixed-valence species with rapidly hopping electrons at room temperature ($k = 1.1 \times 10^{10}$-3.3×10^{11} s^{-1}) and trapped but partially delocalized electrons ($J = 0.074$-0.135 eV) below ca. 100 K. At 107-157 K, electron transfer in $[P_2W_{15}V^{IV}V_2^{V}O_{62}]^{10-}$ is virtually activationless ($E_a = \sim 0.01$ eV). ESR spectra of mixed-valence V_2 and protonated V_3 species are identical at low temperatures and show superhyperfine structure consistent with 5-10% electron delocalization on to the neighboring V(V) atoms. On the basis of the analysis of the intervalence bands of the three mixed-valence complexes, the high-temperature activation energy, E_{th}, is greater for the trinuclear species than for the binuclear as predicted from a recent theoretical model. The stereoisomer of α_2-V (α_1-$[P_2W_{17}VO_{62}]^{8-}$) has also been prepared and characterized. Separation of a mixture of α_1- and α_2-isomers has been achieved by chromatography on modified Sephadex.

It is generally agreed that partial reduction of heteropolymolybdate and -tungstate anions leads to mixed-valence complexes (heteropoly blues) that belong to class II of the Robin-Day scheme.[2,3] Such complexes are therefore described in terms of trapped electrons (Mo^{5+} or W^{5+} centers) that undergo thermal or optical excitation to neighboring Mo^{6+} or W^{6+} sites. A satisfactory quantitative description of these complexes must include magnitudes of activation energies, electron-transfer rates, and

(1) From the Ph.D. Theses of S.P.H. (Georgetown University, 1982) and M.A.L. (Georgetown University, in preparation). A preliminary account of some of this work has been published: Harmalker, S. P.; Pope, M. T. *J. Am. Chem. Soc.* **1981**, *103*, 7381.
(2) Robin, M. B.; Day, P. *Adv. Inorg. Chem. Radiochem.* **1967**, *10*, 247. Day, P. *Int. Rev. Phys. Chem.* **1981**, *1*, 149.
(3) Prados, R. A.; Pope, M. T. *Inorg. Chem.* **1976**, *15*, 2547. Che, M.; Fournier, M.; Launay, J. P. *J. Chem. Phys.* **1979**, *71*, 1954. Launay, J. P.; Fournier, M.; Sanchez, C.; Livage, J.; Pope, M. T. *Inorg. Nucl. Chem. Lett.* **1980**, *16*, 257. Sanchez, C.; Livage, J.; Launay, J. P.; Fournier, M.; Jeannin, Y. *J. Am. Chem. Soc.* **1982**, *104*, 3194.

0002-7863/83/1505-4286$01.50/0

electron delocalization parameters (so-called electron-transfer integrals).

Most theoretical treatments[4,5] of class II systems have focussed on the binuclear case since it is the simplest and because it can be viewed as a model of the activated complex in an electron-transfer reaction. While such treatments appear to be successful for real binuclear systems,[6] they are undoubtedly inadequate even for the most symmetrical of heteropoly blue anions in which each metal atom has four nearest neighbors. In order to simplify the problem, we have synthesized heteropolytungstates in which two or three *adjacent* tungsten atoms have been replaced by vanadium. Reduction of these tungstovanadates allows us to isolate mixed-valence (V^{4+}–V^{5+}) behavior between specific metal sites in a large polyanion structure and to begin to identify preferred "pathways" for electron hopping and delocalization in nonsubstituted polyanions. Such processes in large polyanions become comparable to semiconduction in "infinite" oxide lattices. The present paper describes mixed-valence behavior involving groups of edge-shared VO_6 octahedra. A subsequent paper will discuss complexes in which the VO_6 octahedra share vertices.

Experimental Section

Preparation of Complexes. The lacunary anion salts potassium α_2-heptadecatungstodiphosphate, (α_2-$K_{10}P_2W_{17}O_{61}\cdot 7H_2O$), lithium potassium α_1-heptadecatungstodiphosphate (α_1-$LiK_9P_2W_{17}O_{61}\cdot nH_2O$), and sodium "$\alpha$-hexadecatungstodiphosphate" ("P_2W_{16}") were prepared as described by Contant and Ciabrini.[7] There is some doubt about the true stoichiometry of the last salt, which was used only as an intermediate in the following syntheses.

Potassium α_2-Heptadecatungstovanado(IV)diphosphate (α_2-$P_2W_{17}V$). A solution of 3.3 g of $VOSO_4$ in 200 mL of acetate buffer, pH 4.7, was treated with 50 g of α_2-$K_{10}P_2W_{17}O_{61}$(aq), and the resulting solution deposited dark blue crystals after 2 days. These were recrystallized from hot water. Anal. Calcd for $K_8P_2W_{17}VO_{62}\cdot 10H_2O$: K, 6.6; P, 1.31; W, 66.17; V, 1.08. Found: K, 6.5; P, 1.29; W, 66.25; V, 1.11.

Potassium α_1-Heptadecatungstovanado(IV)diphosphate (α_1-$P_2W_{17}V$). A solution of 2.0 g of $VOSO_4$ in 200 mL of lithium acetate buffer, pH 4.7, was treated with 40 g of $LiK_9P_2W_{17}O_{61}$(aq) and to the resulting purple solution was added saturated KCl to precipitate the desired salt which was washed with 1 M KCl and recrystallized from hot water. Anal. Calcd for $K_8P_2W_{17}VO_{62}\cdot 10H_2O$: K, 6.6; P, 1.31; W, 66.17; V, 1.08. Found: K, 6.5; P, 1.30; W, 66.4; V, 1.05. The product was subsequently discovered to be a mixture of ca. 70% α_1 and 30% α_2 isomers which were separated on a Sephadex column as described in the Appendix.

Potassium α-hexadecatungstodivanado(IV,V)diphosphate ($P_2W^{16}V_2$) and ammonium α-pentadecatungstotrivanado(IV,V,V)diphosphate ($P_2W_{15}V_3$) were both isolated from the same reaction. A solution of 2.0 g of $VOSO_4\cdot H_2O$ in 50 mL of sodium acetate buffer, pH 4.7, was treated with 7.0 g of "P_2W_{16}" (V/P_2 = 3:1) to yield a brownish red solution. A crude sample of $P_2W_{15}V_3$ (contaminated with $P_2W_{16}V_2$) was obtained dropwise addition of 1 M NH_4Cl until precipitation was complete. After filtration (the filtrate contained $P_2W_{16}V_2$ and α_2-$P_2W_{17}V$ anions), the precipitate was dissolved in water and oxidized by dropwise addition of bromine water to a green color. The $P_2W_{16}V_2$ impurity was destroyed by the addition of NaOH to pH 11 and the solution treated dropwise with 1 M NH_4Cl until complete precipitation. The precipitate was washed with 1 M NH_4Cl and dissolved in 0.5 M sodium acetate buffer, pH 4.7, and the solution fully oxidized (orange) with bromine water. After removal of excess bromine by warming, the solution was reduced on a carbon cloth cathode at +0.15 V vs. Ag/AgCl. The product was precipitated with NH_4Cl and recrystallized from hot water. Anal. Calcd for $(NH_4)_8H_2P_2W_{15}V_3O_{62}\cdot 5H_2O$: N, 2.66; P, 1.50; W, 65.6; V, 3.64. Found: N, 2.70; P, 1.48; W, 66.8; V, 3.64; Na, 0.02; K, <0.007.

The filtrate from the original reaction mixture was treated dropwise with 1 M KCl until precipitation was complete. The precipitate was washed with KCl, dissolved in water, and reprecipitated with 1 M KCl. The second precipitate was washed and recrystallized from hot water to yield $P_2W_{16}V_2^{IV}$. Ten grams of the product was dissolved in 100 mL of 0.5 M sodium acetate buffer, pH 4.7, oxidized with bromine water as above, and electrolytically reduced at +0.3 V. The resulting green solution was precipitated with 1 M KCl and the product recrystallized from hot water. Anal. Calcd for $K_9P_2W_{16}V_2O_{62}\cdot 12H_2O$: K, 7.52; P, 1.33; W, 63.0; V, 2.18. Found: K, 7.69; P, 1.29; W, 62.7; V, 2.15.

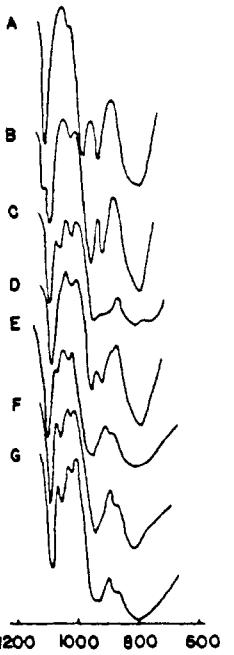

Figure 1. Infrared spectra, in KBr pellets, of salts of A, α-$[P_2W_{18}O_{62}]^{6-}$, B, α_1-$[P_2W_{17}VO_{62}]^{8-}$, C, α_2-$[P_2W_{17}O_{61}]^{10-}$, D, α_2-$[P_2W_{17}VO_{62}]^{8-}$, E, $[P_2W_{16}V_2O_{62}]^{9-}$, F, $[HP_2W_{15}V_3O_{62}]^{9-}$ (salt isolated at pH 4.7), and G, $[P_2W_{15}V_3O_{62}]^{10-}$ (salt isolated at pH 11.0).

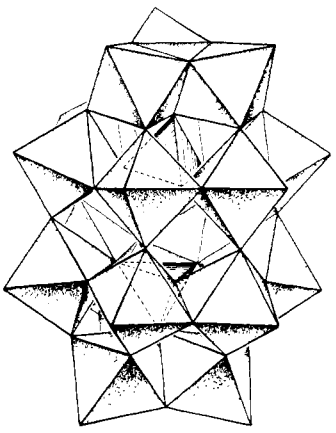

Figure 2. Structure of α-$[P_2W_{18}O_{62}]^{6-}$ as an assembly of PO_4 and WO_6 polyhedra.

Analyses. Vanadium was determined by redox titration with iron(II)[8] and tungsten as the oxinate.[9] Other analyses were done by Galbraith Laboratories, Knoxville, TN.

Physical Measurements. Optical and vibrational spectra and electrochemical measurements were made as described earlier.[10] X-band ESR spectra were recorded on JEOL ME-3X, Varian E-9, and EC-102 spectrometers. Spectra were simulated by using the program CURHEPR.[11] Vanadium-51 (23.67 MHz) and phosphorus-31 (36.44 MHz) NMR spectra were recorded in pulse FT mode on a Bruker WH-90 spectrometer using a wide-band multinuclear probe and quadraphase detection. Samples, using D_2O as a source of lock signal, were contained in spinning 10-mm tubes. Further details are given below.

(4) Hush, N. S. *Prog. Inorg. Chem.* **1967**, *8*, 391. "Mixed-Valence Compounds"; Brown, D. B., Ed.; D. Reidel: Dordrecht, 1980; p 151.

(5) Piepho, S. B.; Krausz, E. R.; Schatz, P. N. *J. Am. Chem. Soc.*, **1978**, *100*, 2996. Wong, K. Y.; Schatz, P. N.; Piepho, S. B. *Ibid.* **1979**, *101*, 2793. Wong, K. Y.; Schatz, P. N. *Prog. Inorg. Chem.* **1981**, *28*, 369.

(6) Several examples are given in "Mixed-Valence Compounds"; Brown, D. B., Ed.; D. Reidel, Dordrecht, 1980.

(7) Contant, R.; Ciabrini, J. P. *J. Chem. Res., Synop.* **1977**, 222; *J. Chem. Res. Miniprint* 2601.

(8) Flynn, C. M., Jr.; Pope, M. T. *Inorg. Chem.* **1971**, *10*, 2524.

(9) Erdey, L. "Gravimetric Analysis"; Pergamon Press: Oxford, 1965; Vol. II.

(10) Varga, G. M., Jr.; Papaconstantinou, E.; Pope, M. T. *Inorg. Chem.* **1970**, *9*, 662. Prados, R. A.; Pope, M. T. *Ibid.* **1976**, *15*, 2547.

(11) Venables, J.; Brill, A. S. University of Virginia, private communication.

Table I. ^{31}P and ^{51}V NMR Data for Tungstovanadophosphates[a] at pH 4.7

anion	$\delta(^{31}P)^b$	$\delta(^{51}V)^c$	$\Delta\nu_{1/2}(^{51}V)^d$
α-$[P_2W_{18}O_{62}]^{6-}$	−12.7[e]		
α_1-$[P_2W_{17}VO_{62}]^{7-}$	−12.3, −13.4	−570	180
α_2-$[P_2W_{17}VO_{62}]^{7-}$	−11.4, −13.5	−554.7	33
α-$[P_2W_{16}V_2O_{62}]^{8-}$	−9.3, −13.9	−528	70
α-$[P_2W_{15}V_3O_{62}]^{9-}$	−6.8, −14.4	−503[f]	130[f]

[a] Ca. 0.01 M heteropolyanion, 0.25 M acetate buffer, 50% D_2O. ^{31}P: 36.44 MHz; pulse width, 5 μs; sweep width, 2 KHz; 4K data points; delay, 500; repetition rate, 3–30 s, see text; number of transients, 2100–13 785. ^{51}V: 23.67 MHz, pulse width, 3.1 μs; sweep width, 20 KHz; 4K data points, delay, 50; repetition rate, 0.2 s; number of transients, 13 950–30 258. [b] Positive chemical shift (±0.2) in ppm downfield from 85% H_3PO_4. [c] Positive chemical shift (±2) in ppm downfield from $VOCl_3$. [d] Line width at half-height (Hz, uncertainty ±15% of value given), measured at ca. 30 °C. [e] Reference 16. [f] Chemical shift and line width are pH dependent (pH, δ ($\Delta\nu$)): 4.0, −506 (135); 3.5, −513 (190); 2.5, −537 (260).

Results and Discussion

Vibrational and NMR Spectra. The IR spectra of the tungstovanadates in the P–O, M–O stretching region are shown in Figure 1 along with those of α-$[P_2W_{18}O_{62}]^{6-}$ and α_2-$[P_2W_{17}O_{61}]^{10-}$. The similarity of the spectra of all 18-nucleate anions strongly indicates that they have the same structure as α-$[P_2W_{18}O_{62}]^{6-}$ (Figure 2). The latter anion has virtual D_{3h} symmetry with six "polar" and 12 "equatorial" tungstens.[15] The lacunary anions $[P_2W_{17}O_{61}]^{10-}$ are known to have the same structure minus a WO^{4+} group, lost from a polar site (α_2-isomer[12,13]) or from an equatorial site (α_1-isomer[14]). We can therefore conclude that α_1- and α_2-$[P_2W_{17}VO_{62}]^{7-}$ anions have vanadium atoms in equatorial and polar sites, respectively.

Phosphorus-31 and vanadium-51 NMR data are presented in Table I for solutions of the tungstovanadates at pH 4.7 oxidized to the V^{5+} state with bromine water. The NMR results confirm the above structural assignments for α_1- and α_2-$P_2W_{17}V$ and demonstrate that $P_2W_{16}V_2$ and $P_2W_{15}V_3$ are unique species with vanadium atoms occupying one of the polar groups of P_2W_{18}. We note first that each PWV anion gives two phosphorus and one vanadium resonance as expected. The vanadium resonance line widths are instructive, since they are dominated by interaction of the quadrupole moment, Q, and electric field gradient, q, of the ^{51}V nucleus. For a molecule undergoing spherical rotation

$$\Delta\nu_{1/2} = \frac{3\pi}{10}\left(\frac{2I+3}{I^2(2I-1)}\right)\left(1+\frac{\eta^2}{3}\right)\left(\frac{e^2q_{zz}Q}{h}\right)^2\tau_c$$

where η is the so-called asymmetry parameter ($= (q_{yy} - g_{xx})/q_{zz}$), τ_c is the molecular rotational correlation time, and the other symbols have their usual meanings. The correlation times of isostructural heteropolyanions in the same solvent at the same temperature will be identical, and therefore the different line widths in Table I, for equimolar solutions, reflect differences in the magnitudes of η and q. The much broader line of α_1-$P_2W_{17}V$ compared with that of the α_2-isomer can be understood in terms of the lower symmetry of an equatorial vs. a polar MO_6 octahedron. Although it is probably impossible to partition the effects of η and q in this case, the broader line for α_1 might formally be attributed to an increased η value caused by the presence of almost linear M–O–M bonds (162° in P_2W_{18}[15]) that link the two halves of the anion and imply greater π bonding in that direction. The line widths of $P_2W_{16}V_2$ and $P_2W_{15}V_3$, although greater[17] than that of α_2-$P_2W_{17}V$, are nevertheless narrower than that of the α_1-isomer, from which we can conclude that the former two anions do not contain vanadiums in equatorial sites. The ^{31}P spectra show a gradual progression of chemical shifts as the number of vanadium atoms increases. The upfield line (at ca. −14 ppm) is assigned to the phosphorus atom in the unsubstituted half of the anion for three reasons: (1) The total change of δ from P_2W_{18} to $P_2W_{15}V_3$ is less than 2 ppm (contrast with ~6 ppm for the other line). (2) The line shifts further *upfield* upon substitution by vanadium, whereas the other line shifts downfield, as do the ^{31}P resonances in the series $[PW_{12}O_{40}]^{3-}$ (−14.96 ppm), $[PW_{11}VO_{40}]^{4-}$ (−14.80 ppm), $[PW_{10}V_2O_{40}]^{5-}$ (−13.9 to −14.3 ppm), $[PV_{14}O_{42}]^{9-}$ (+1 ppm).[18,19] The downfield shift is attributed to an increase of P–O π bonding when the atom sequence P–O–W is replaced by P–O–V. (3) The line always appeared less intense than the other unless the delay between pulses was increased to 30 s. We conclude that the phosphorus nucleus responsible for the downfield line is undergoing faster relaxation because it is more strongly coupled to the nearby vanadium atom(s).

Further confirmation of the vanadium positions in $P_2W_{16}V_2$ and $P_2W_{15}V_3$ is provided by the ESR parameters which are discussed later.

Table II. Voltammetric Data for Vanadium Redox Processes in Tungstovanadodiphosphates[a]

anion	pH, counterion[b]	cathodic peak potentials[c]
α_1-$P_2W_{17}V$	4.7, Na^+	+0.51 (1)[d]
	5.5, Li^+	+0.48 (1)
α_2-$P_2W_{17}V$	4.7 Na^+	+0.41 (1)
	5.5 Li^+	+0.39 (1)
$P_2W_{16}V_2$	5.5 Li^+	+0.27 (1), +0.08 (1)
$P_2W_{15}V_3$	5.5 Li^+	+0.23 (1), + 0.06 (2)
	7.0 Li^+	+0.11 (1), −0.08 (1), −0.32 (1)

[a] Glassy carbon electrode, 1 V min^{-1}. [b] Supporting electrolyte 0.5 M acetate buffer or 1.0 M acetate (pH 7.0). [c] V vs. Ag/AgCl, uncertainty ±0.02 V. [d] Number of electrons, confirmed by controlled potential coulometry in each case.

Table III. Electronic Absorption Band Positions and Intensities of Oxidized Tungstovanadodiphosphates at pH 4.7

anion	approx band position[a] (extinction coefft[b])
α_1-$P_2W_{17}V$	24 300 (1500), 33 000 (35 000), 39 000 (58 000)
α_2-$P_2W_{17}V$	23 800 (1600), 33 000 (35 000), 39 000 (58 000)
$P_2W_{16}V_2$	23 000 (2100), 34 000 (35 000), 39 000 (50 000)
$P_2W_{15}V_3$	22 500 (2800), 37 000 (50 000)

[a] All spectra consisted of a series of poorly resolved shoulders. Energies in cm^{-1}. [b] M^{-1} cm^{-1}.

Electrochemistry. Cyclic voltammograms of the tungstovanadates using a glassy carbon electrode showed a series of reversible one- and two-electron redox processes as summarized in Table II. Not shown in the table are the peak potentials for reduction of the tungsten atoms in each ion. The latter processes, which were not studied in detail, appear as two- and four-electron steps at negative potentials.[20] The redox potentials of the $P_2W_{17}V$ isomers are noteworthy since they confirm that the equatorial sites in the P_2W_{18} structure are more easily reduced than the polar sites.[10] Similarly, the corresponding isomers of $P_2W_{17}Mo$ have $Mo^{6+/5+}$ reduction potentials that differ by 200 mV (α_1 more positive),[7] and the heteropoly blue anion $[H_2P_2Mo_2{}^{V}Mo_{16}O_{62}]^{6-}$ appears to have two of the equatorial Mo atoms reduced.[21,22]

(12) Kazanskii, L. P. *Koord. Khim.* **1976**, *2*, 719.
(13) Acerete, R.; Harmalker, S.; Hammer, C. F.; Pope, M. T., Baker, L. C. W. *J. Chem. Soc., Chem. Commun.* **1979**, 777.
(14) Rocchiccioli-Deltcheff, C.; Thouvenot, R. *Spectrosc. Lett.* **1979**, *12*, 127.
(15) Dawson, B. *Acta Crystallogr.* **1953**, *6*, 113. D'Amour, H. Acta Crystallogr. *Sect. B.* **1976**, *B32*, 729.
(16) Massart, R.; Contant, R.; Fruchart, J. M.; Ciabrini, J. P.; Fournier, M. *Inorg. Chem.* **1977**, *16*, 2916.
(17) The ^{51}V line widths decrease by about 70% as the temperature is raised from 30 to 80 °C. This occurs for all the anions as the solvent viscosity and τ_c are diminished. The greater line widths of V_2 and V_3 anions compared to α_2-V probably reflect changes in η and q caused by V–O–V bond sequences.
(18) O'Donnell, S. E.; Pope, M. T. *J. Chem. Soc., Dalton Trans.* **1976**, 2290.
(19) Kato, R.; Kobayashi, A.; Sasaki, Y. *Inorg. Chem.* **1982**, *21*, 240.
(20) Cathodic peak potentials for tungsten reductions at pH 4.7, in V vs. silver/silver chloride: α_1-$P_2W_{17}V$; −0.42, −0.73, −1.0; α_2-$P_2W_{17}V$, −0.51, −0.70, −0.94; $P_2W_{16}V_2$, −0.60, −0.70, −0.90; $P_2W_{15}V_3$, −0.70, −0.84.
(21) Garvey, J. F.; Pope, M. T. *Inorg. Chem.* **1978**, *17*, 1115.

Table IV. Electronic Absorption Band Positions and Intensities of Reduced Tungstovanadodiphosphates[a]

anion	band position[b] (extinction coeff)
α_1-$P_2W_{17}V^{IV}$	13 300 sh (450), 14 700 sh (575), 19 000 (720), 22 500 sh (575)
α_2-$P_2W_{17}V^{IV}$	13 000 sh (450), 14 700 sh (575), 16 600 (680), 23 500 sh (575)
$P_2W_{16}V_2^{IV}$	11 500 sh (175), 14 500 sh (425), 20 000 (1105)
$P_2W_{16}V^{IV}V^{V}$	8500 (400), 11 500 sh (500), 19 000 (650)
$P_2W_{15}V_3^{IV}$	11 600 sh (110), 15 000 sh (400), 21 000 (1275)
$P_2W_{15}V^{IV}V_2^{V}$	8700 (690), 11 500 (910), 13 000 sh (880), 15 000 sh (775), 19 000 sh (650)
$P_2W_{15}V^{IV}V_2^{V}$ *c*	~9000 sh (200),[d] 13 000 sh (750), 13 700 (825), 15 000 sh (780), 19 000 sh (650)

[a] Acetate buffer, pH 4.7 except where noted. [b] cm^{-1}, sh = shoulder. Extinction coefficient in M^{-1} cm^{-1}. [c] pH 11.0. [d] Band uncertain.

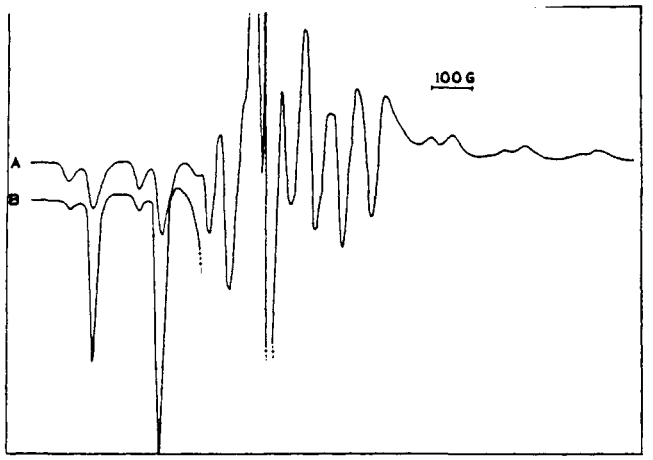

Figure 3. X-band ESR spectrum of a mixture of α_1- and α_2-$[P_2W_{17}VO_{62}]^{8-}$ in water–glycerol glass, pH 4.7, at 77 K. The lower trace shows the spectrum of a purified sample of the α_1-isomer (see Appendix).

Electronic Spectra. The optical absorption spectra of all the anions in oxidized (V^V), reduced (V^{IV}), and mixed-valence states are summarized in Tables III and IV. The poorly defined absorption bands listed in Table III are assigned to $O \rightarrow V^V$ (<25 000 cm^{-1}) and $O \rightarrow W^{VI}$ (>30 000 cm^{-1}) charge-transfer transitions. The spectra of the reduced complexes (Table IV) contain d–d transitions of V^{IV} (11 500–15 000 cm^{-1}) and intervalence charge-transfer (IT) transitions, $V^{IV} \rightarrow V^V$ (8500 cm^{-1}) and $V^{IV} \rightarrow W^{VI}$ (16 600–23 500 cm^{-1}). Except for the V^{IV}–V^V IT bands, these assignments must be regarded as provisional. Other investigations of the spectra of reduced polyanions have assigned the *two* lowest energy bands as homonuclear ($Mo^V \rightarrow Mo^{VI}$; $W^V \rightarrow W^{VI}$) IT transitions.[3,23] In the present work the second band, at 11 500 cm^{-1}, appears also in the spectra of the fully reduced $P_2W_{16}V_2^{IV}$ and $P_2W_{15}V_3^{IV}$ anions and cannot be caused solely by $V^{IV} \rightarrow V^V$. The IT band(s) of $P_2W_{15}V^{IV}V_2^{V}$ at high pH will be discussed below.

Electron Spin Resonance. The X-band ESR spectra of α_1- and α_2-$P_2W_{17}V^{IV}$ in aqueous buffer at ~350 K or in water–glycerol glass at 77 K show the expected hyperfine interaction with the vanadium-51 nucleus (99.75%, $I = {}^7/_2$). The *g* and *a* parameters listed in Table V were obtained by simulation of the experimental spectra and are based on the customary spin Hamiltonian for an axial d^1 ion. Also shown in Table V are data for other tungstovanadates, as well as Kazanskii's results[12] for α_2-$P_2W_{17}V^{IV}$ which are seen to be in fair agreement with ours. Kazanskii had correctly concluded from the similarity of their ESR parameters that the vanadium atoms in $P_2W_{17}V^{IV}$ and $PW_{11}V^{IV}$ occupied one of the MO_6 octahedra in the edge-shared M_3O_{13} group common to both structures. The second (α_1) isomer of $P_2W_{17}V$ had not been prepared at the time of Kazanskii's work, and it was not known whether the isomers would have sufficiently different ESR parameters to render this conclusion valid. We can not see that the *g* values (especially $g_\parallel$) are quite different for the two isomers and mixtures of the isomers are readily analyzed by ESR at 77 K (see Figure 3). The *g* values for tetragonal $V^{IV}OL_5$ complexes (C_{4v} symmetry) may be approximated by the equations[26]

$$g_\parallel = 2.0023 - \frac{8\alpha^2\beta^2\lambda}{\Delta E(B_2 \rightarrow B_1)} \quad (1)$$

$$g_\perp = 2.0023 - \frac{2\alpha^2\gamma^2\lambda}{\Delta E(B_2 \rightarrow E)} \quad (2)$$

where α^2, β^2, and γ^2 are respectively the fractional contributions of d_{xy}, $d_{x^2-y^2}$, and d_{xz}, d_{yz} orbitals to the ligand field b_2, b_1, and e molecular orbitals, λ is the spin–orbit coupling parameter for the metal ion, and the denominators are the energies of the ligand field transitions. The factor of 8 in the expression for $g_\parallel$ is responsible for the greater variability observed for $g_\parallel$ over $g_\perp$. We note from Table V that $g_\parallel$ diminishes in the sequence $[VW_5O_{19}]^{4-} > [PW_{11}VO_{40}]^{5-} \approx \alpha_2$-$[P_2W_{17}VO_{62}]^{8-} > \alpha_1$-$[P_2W_{17}VO_{62}]^{8-}$ and suggest that this variation may be accounted for qualitatively by considering changes in the in-plane bonding of the vanadium atom. The π contribution to this bonding is reflected in the magnitude of the bond angles V–O–W, which vary from ~120° to ~155° in the four heteropolyanions. The larger angles occur between VO_6 and WO_6 octahedra that share a common vertex rather than those that share an edge. We make the empirical observation that $g_\parallel$ diminishes as the VO_6 octahedron increases its number of vertex-shared contacts from none in $[VW_5O_{19}]^{4-}$ to three in α_1-$[P_2W_{17}VO_{62}]^{8-}$. It would of course be unwise to attempt to blame this change upon any *one* of the parameters of eq 1 since they are all interrelated. Furthermore, eq 1 and 2 are only strictly

Table V. ESR Parameters[a] for Some Tungstovanadates

anion	⟨*g*⟩	⟨*a*⟩	$g_\parallel$	$g_\perp$	$A_\parallel$	$A_\perp$	ref
$[VW_5O_{19}]^{4-}$	1.962		1.949	1.969			24
α-$[PW_{11}VO_{40}]^{5-}$	1.952		1.915	1.970	187	65	25
α_2-$[P_2W_{17}VO_{62}]^{8-}$	1.952	98.7	1.917	1.970	180	58	this work
			1.928	1.978			12
α_1-$[P_2W_{17}VO_{62}]^{8-}$	1.937	95	1.885	1.964	180	52	this work

[a] Hyperfine values in gauss.

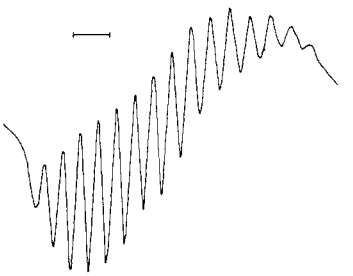

Figure 4. X-band ESR spectrum of $P_2W_{16}V^{IV}V^V$ in aqueous acetate buffer, pH 4.7 (temperature, 80 °C; scale bar, 100 G).

(22) Kazansky, L. P.; Fedotov, M. A. *J. Chem. Soc., Chem. Commun.* **1980**, 644.
(23) Fruchart, J. M.; Herve, G.; Launay, J. P.; Massart, R. *J. Inorg. Nucl. Chem.* **1976**, *38*, 1627.
(24) So, H.; Flynn, C. M., Jr.; Pope, M. T. *J. Inorg. Nucl. Chem.* **1974**, *36*, 329.
(25) Smith, D. P.; So, H.; Bender, J.; Pope, M. T. *Inorg. Chem.* **1973**, *12*, 685.
(26) DeArmond, K.; Garrett, B. B.; Gutowsky, H. S. *J. Chem. Phys.* **1965**, *42*, 1019.

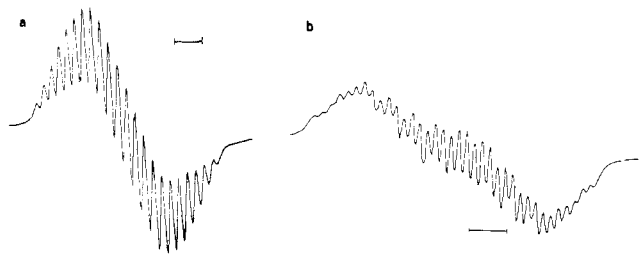

Figure 5. X-band ESR spectra of $P_2W_{15}V^{IV}V_2^V$ in aqueous solution at ca. 80 °C: (a) pH 11.0; (b) pH 4.7 (scale bars, 100 G).

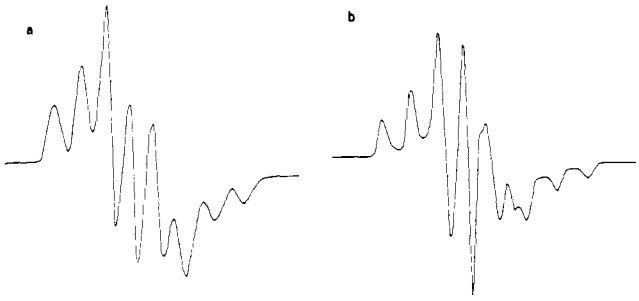

Figure 6. X-band ESR spectra of $P_2W_{15}V^{IV}V_2^V$ in water–glycerol glass at 77 K: (a) pH 4.7; (b) pH 11.0.

valid for $[VW_5O_{19}]^{4-}$ in which the vanadium atom has C_{4v} symmetry.

The ESR spectra of the mixed valence ions $P_2W_{16}V^{IV}V^V$ and $P_2W_{15}V^{IV}V_2^V$ show that at room temperature and above the unpaired electron interacts with more than one ^{51}V nucleus. Solution spectra recorded at ~80 °C for optimum resolution[27] are shown in Figures 4 and 5. The spectrum of the divanadate consists of 15 lines (a = 50 ± 1 G; g = 1.961 ± 0.002) and is unchanged between pH 4.0 and 10.0. The spectrum of the trivanadate consists of 22 equally spaced lines (a = 33 ± 1 G; g = 1.953 ± 0.002) at pH 11.0 but is more complex at pH 4.7 with 36 equally spaced lines (a = 21.2 ± 0.5 G). The two spectra were found to be reproducibly interconverted at pH ~9. Titration of a solution of $H_{10}P_2W_{15}V^{IV}V_2^VO_{62}$, prepared by ion exchange from the ammonium salt, with 0.1 M NaOH revealed endpoints at 8.9 ± 0.1 and 9.8 ± 0.2 equiv of OH^-/mol of heteropolyanion. The estimated pK of the second step is 8 in fair agreement with the ESR results. We therefore attribute the 22-line spectrum to $[P_2W_{15}V^{IV}V_2^VO_{62}]^{10-}$ and the 36-line spectrum to $[HP_2W_{15}V^{IV}V_2^VO_{62}]^{9-}$. The expected intensity ratios of the components of the 15-line (1:2:3:4...7:8:7...2:1) and 22-line spectra (1:3:6:10:15:21:28:36:42:46:48:48:46...6:3:1) are approximately matched by the experimental spectra when due consideration is made for variation in line width caused by slow tumbling of the large anisotropic anions. There are two possible explanations for a 36-line spectrum involving three $I = {}^7/_2$ nuclei: (1) eight lines (a_8 = 3 × 21 G) each split into 15 (a_{15} = 21 G); and (2) 15 lines (a_{15} = 2 × 21 G) each split into eight (a_8 = 21 G). The expected relative intensities are, to first order, as follows: (1) 1:2:3:5:7:9:12:15:16:18:20:20:21:22:21:21:22:21| 21:22...3:2:1 and (2) 1:1:3:3:6:6:10:10:14:14:18:18:22:22:26:26:28:28| 28:28...3:3:1:1. The experimental spectrum is seen to be in closer agreement with case 1 than with case 2. When recorded at lower temperatures in 50% water–glycerol glasses, the ESR spectra showed a gradual coalescence to "normal" anisotropic forms typical of mononuclear vanadium(IV) but with somewhat broader lines than usual; see Figure 6. At 77 K and below the spectra of $P_2W_{16}V_2$ and $HP_2W_{15}V_3$ were identical. Spin Hamiltonian parameters, confirmed by simulation of the 77 K spectra using Gaussian lines of width 30 G, are given in Table VI.

The behavior illustrated by Figures 4–6 clearly establishes that the tungstovanadates are class II mixed-valence complexes in

Table VI. ESR Parameters[a] for Mixed-Valence Tungstovanadates at 77 K

anion	$g_\parallel$	$g_\perp$	$A_\parallel$	$A_\perp$
$[P_2W_{15}V_2O_{62}]^{9-}$ and $[HP_2W_{16}V_3O_{62}]^{9-}$	1.944	1.97_0	149	78
$[P_2W_{15}V_3O_{62}]^{10-}$	1.927	1.76_7	160	70

[a] Hyperfine values in gauss.

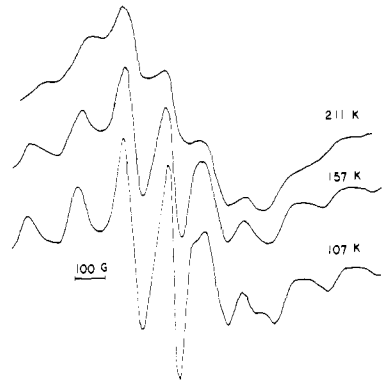

Figure 7. Temperature variation of the ESR spectrum of $P_2W_{15}V^{IV}V_2^V$ in water–glycerol glass, pH 11. The spectrum is unchanged between 107 and 5 K.

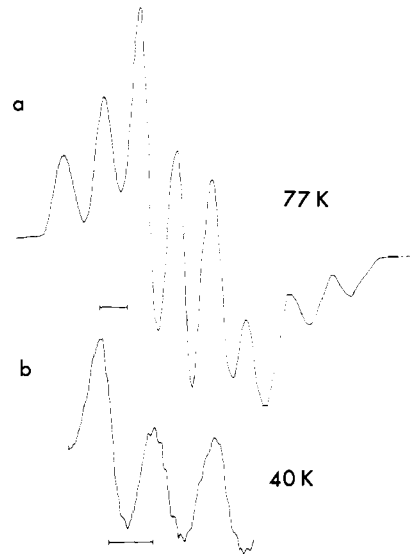

Figure 8. X-band ESR spectra of $P_2W_{16}V^{IV}V^V$ and $HP_2W_{15}V^{IV}V_2^V$ in glycerol glass, pH 4.7: upper trace, 77 K; lower trace, expanded central portion of spectrum at 40 K showing superhyperfine structure. The spectra could not be recorded at temperatures lower then 40 K owing to saturation of the signal. (scale bars, 100 G).

which the unpaired electrons are trapped[28] on a single vanadium atom at 77 K. The broad lines of the 77 K spectra may indicate either that intramolecular electron transfer (hopping) is still occurring at that temperature or that partial delocalization of the trapped electron to the neighboring V^V atom(s) has given rise to (unresolved) superhyperfine structure. The second interpretation appears to be correct for the reasons presented in the following paragraph.

The ESR spectrum of $P_2W_{15}V_3$ is unchanged between 5 and 77 K; further line broadening, indicating that the rate of electron hopping approaches 10^8 s^{-1}, only appears at temperatures above ~100 K; see Figure 7 and discussion below. The (identical) spectra of $P_2W_{16}V_2$ and $HP_2W_{15}V_3$ can be observed only at temperatures above ~40 K; at lower temperatures the signals saturate,

(27) At lower temperatures the lines broaden as a result of slow molecular tumbling, see: Harmalker, S. P.; Pope, M. T. *J. Phys. Chem.* **1978**, *82*, 2823.

(28) "Trapped" on the ESR time scale implies a residence time on one nucleus ≫ s.

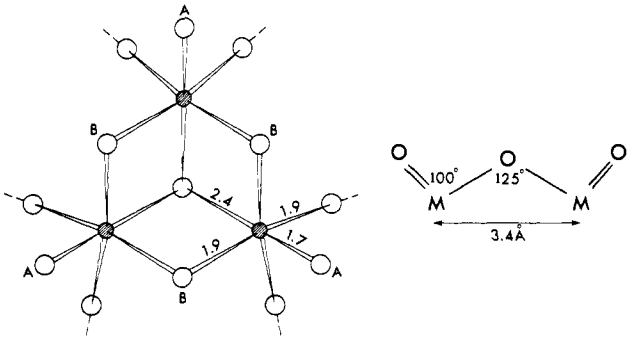

Figure 9. Dimensions of the M_3O_{13} group of three edge-shared WO_6 octahedra in α-$[P_2W_{18}O_{62}]^{6-}$ taken from ref 15. The sequence of atoms O_A–M–O_B–M–O_A are virtually coplanar with approximate bond lengths and angles shown. These values are not expected to change greatly as W^{6+} is replaced by V^{5+} in the group.[29]

even under conditions of low microwave power. However, as shown in Figure 8, at 40–50 K the spectra show reproducible superhyperfine features on the central, most intense lines. The new features are defined by a splitting constant, $a_{SHF} \approx 10$ G. To our knowledge this is the first example of a class II mixed-valence species in which *direct observation* of partial delocalization of a trapped electron has been made. The magnitude of a_{SHF} indicates about 5–10% delocalization on the basis of typical a values for mononuclear vanadium complexes.

Interpretation of ESR Spectra. The approximate dimensions of one of the polar groups of three edge-shared MO_6 octahedra in α-$[P_2M_{18}O_{62}]^{6-}$, taken from D'Amour's X-ray investigation of the tungstate,[15] are are given in Figure 9. Bond lengths and angles are unlikely to be very much different when one or more of the three tungsten(VI) atoms are replaced by vanadium(V).[29] With the assumption that each VO_6 octahedron has approximately C_{4v} symmetry with the z axis defined by the terminal V=O bond, the unpaired electron occupies a d_{xy} orbital. We represent the three heteropolyanion structures by the abbreviated forms.

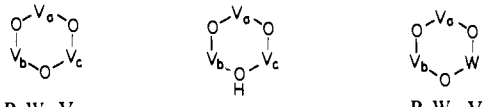

We assume that electron hopping in the mixed-valence complexes occurs via the oxygen atoms shown; the process can be viewed as an intramolecular bridged electron transfer. Since the unpaired electron on V^{4+} occupies an orbital that has π symmetry with respect to the bridging V–O bonds, it is to be expected that electron transfer will be facilitated as the π bond order of the V–O–V bonds increases. In these structures the extent of V–O–V π bonding is low as a result of the $\sim$125° bridge bond angle. As a result, electron trapping occurs at relatively high temperatures.

In the cases of $P_2W_{15}V_3$ and $P_2W_{16}V_2$ at high temperatures, the 22- and 15-line spectra show the vanadium atoms to be equivalent on the ESR time scale, as required by the molecular symmetries of C_{3v} and C_s respectively. When the electron becomes trapped on one of the vanadium atoms of $P_2W_{16}V_2$, all molecular symmetry is lost, but it is possible to detect (Figure 8) superhyperfine interaction indicating partial delocalization of spin density on to the second vanadium. Since exactly the same ESR behavior is observed for $HP_2W_{15}V_3$, we assume (1) that protonation of the anion occurs at one of the V–O–V bridging oxygens[30] as shown above, (2) that the electron is trapped on atom V_b or V_c (see below), and (3) that electron delocalization through the V–OH–V bridge is much smaller than through V–O–V. As a result, the same pattern of superhyperfine structure is observed for $HP_2W_{15}V_3$ as for $P_2W_{16}V_2$. When the electron becomes trapped on one of the three (originally equivalent) vanadium atoms of $P_2W_{15}V_3$, the molecular symmetry is reduced to C_s. For an electron trapped on, say, V_a, partial spin density delocalization on to *two* equivalent vanadiums (V_b and V_c) would give rise to more superhyperfine lines (and with smaller splitting) than was observed for $P_2W_{16}V_2$ and $HP_2W_{15}V_3$ anions. We conclude that the broad lines in the low-temperature spectra of $P_2W_{15}V_3$ result from such unresolved superhyperfine structure. The different g and a values for protonated and unprotonated V_3 anions also rule out the possibility that the electron is trapped on V_a of $HP_2W_{15}V_3$ (see assumption 2 above).

Finally, we consider the high-temperature solution spectrum of $HP_2W_{15}V_3$. We invoke the Franck–Condon principle and also assume that electron transfer between V_b and V_c is much slower than between the other pairs of vanadium atoms. Statistically therefore we should expect to see 50% of the electron density on V_a and 25% each on V_b and V_c as a result of fast exchange in the sequence $V_b \rightarrow V_a \rightarrow V_c \rightarrow V_a \rightarrow$ etc. The experimental hyperfine splitting parameters are $\sim$60 G for V_a and $\sim$20 G for V_b and V_c. These values, if they are taken to be approximately proportional to the relative residence times of the unpaired electron on each vanadium atom, are seen to be in reasonable agreement with the statistical model.[31]

Intervalence Spectra and Electron-Transfer Rates. As has been well established,[2,4,5] the parameters of intervalence charge-transfer (IT) bands in the spectra of class II mixed-valence species are related to the rate and activation energy of the electron transfer. For a simple binuclear case ($P_2W_{16}V^{IV}V^{V}$ and, effectively, $HP_2W_{15}V^{IV}V_2^{V}$) the energy of the lowest IT band, E_{op}, is related to the activation energy (E_{th}) for the thermal electron transfer from V^{IV} to V^{V} by the equation $E_{th} = {}^1/_4E_{op}$. This simple formula is however valid only when there is strictly no electron delocalization and when $kT \gg h\omega$ for the molecular vibrations which are coupled to the electron transfer. Neither of these requirements is satisfied by any real class II complex; in the present case $h\omega$ for V–O–V vibrations is 700–800 cm^{-1}. Slight electron delocalization, corresponding to a splitting of the intersection region of the potential energy curves for the "donor" and "acceptor" atoms, may be treated by perturbation theory and leads to the equation[5,32]

$$E_{th} = {}^1/_4E_{op} - J + J^2/E_{op} \qquad (3)$$

J is the so-called electron-transfer integral.[33] The quantity E_{op} in eq 3 contains two components, χ_i and χ_o corresponding to inner-sphere and outer-sphere contributions to the valence trap.[34] The outer-sphere term is approximated by

$$\chi_o = e^2\left(\frac{1}{2a_1} + \frac{1}{2a_2} - \frac{1}{d}\right)\left(\frac{1}{n^2} - \frac{1}{D_s}\right) \qquad (4)$$

where a_1 and a_2 are the radii of the donor and acceptor ions, d is the distance between their centers, n and D_s are respectively the refractive index and the static dielectric constant of the solvent. As shown by Taube and others,[35] a plot of E_{op}, recorded for the same complex in different solvents, vs. $(1/n^2 - 1/D_s)$ is linear with intercept χ_i. In many mixed-valence diruthenium cations χ_i and χ_o ($= E_{op} - \chi_i$) are found to be of similar magnitudes. For the heteropolyanions $P_2W_{16}V^{IV}V^{V}$ and $HP_2W_{15}V^{IV}V_2^{V}$, the absorption

(29) The probability of direct X-ray determination of such differences in bond lengths is low; the substituted ions are likely to retain a crystallographically imposed threefold axis.

(30) In view of the lower oxidation state of vanadium vis-à-vis tungsten, these oxygen atoms are expected to be the most basic sites on the surface of the heteropolyanion. This conclusion is strengthened by ^{17}O NMR results which indicate that the V–O–V oxygen atom is protonated in acetonitrile solutions of $HV_2W_4O_{19}^{3-}$ (Klemperer, W. G.; Shum, W. *J. Am. Chem. Soc.* **1978**, *100*, 4891).

(31) An exact correlation between $\langle a \rangle$ and the electron residence time is not of course to be expected since the two vanadium sites have different local symmetries, g values, etc.

(32) Cannon, R. D. "Electron Transfer Reactions"; Butterworths: London 1980.

(33) This quantity has also been referred to as the electron-tunnelling matrix element, V_{ab} or T_{da}.

(34) Meyer, T. J., ref 6, p 75.

(35) Tom, G. M.; Creutz, C.; Taube, H. *J. Am. Chem. Soc.* **1974**, *96*, 7827. Powers, M. J.; Meyer, T. J. *Ibid.* **1978**, *100*, 4393; **1980**, *102*, 1289.

Table VII. IT Band Parameters and Derived Quantities

	anion		
	$P_2W_{16}V^{IV}V$	$HP_2W_{15}^{-}$ $V^{IV}V_2V$	$P_2W_{15}^{-}$ $V^{IV}V_2V$
E_{op}, cm^{-1}	8500	8700	13 700[a]
$\nu_{1/2}$, cm^{-1}	3600	3900	7000
ϵ_{max}	325	345[b]	350[b]
J, eV	0.074	0.080	0.135
E_{th}, eV	0.195	0.196	0.300
k_{et}, s^{-1}	3.0×10^{11}	3.3×10^{11}	1.3×10^{10}

[a] See text for an alternative assignment and derived quantities. [b] Half of experimental value, i.e., ϵ/V_2 unit.

maxima were found to be virtually the same in water, acetone, acetonitrile, and benzene[36] (solvents for which $1/n^2 - 1/D_s$ varies from 0.546 to 0.005), and hence we conclude that $\chi_o = \sim 0$. This result is not unexpected for large polyanions which are weakly solvated.[37]

In Table VII are presented values of J, E_{th}, and k_{et} (the rate constant for intraionic electron transfer) calculated from the IT band parameters by using eq 3, 5, and 6,[38] where, in (5), $\nu_{1/2}$ and

$$J = ((4.2 \times 10^{-4})\epsilon_{max}\nu_{1/2}E_{op}/d^2)^{1/2} \quad (5)$$

$$k_{et} = (2\pi J^2/h)(\pi/k_bTE_{op})^{1/2} \exp(-E_{th}/RT) \quad (6)$$

E_{op} are in units of 10^3 cm^{-1} and the internuclear separation d is in Å. When considering the significance of the values reported in Table VII, it should be borne in mind that eq 3, 5, and 6 were derived under a number of assumptions some of which, e.g., that the quantum spacings are small compared with kT, are clearly not valid for the heteropolyanions, as mentioned above. The activation energies are apparent high-temperature limits, for semiclassical[39] and vibronic coupling models[5] of electron transfer demonstrate that the concept of a fixed activation energy is evanescent. The activation energy diminishes as the temperature falls since activationless (tunnelling) electron transfer predominates at low temperature. For example, Brunschwig et al.[39] have calculated activation energies for $Fe(H_2O)_6^{2+}/Fe(H_2O)_6^{3+}$ of 6.25 kcal mol^{-1} at 300 K and 0.17 kcal mol^{-1} at 60 K. We can demonstrate a similar effect with the heteropolyanions. The ESR spectrum of $P_2W_{15}V^{IV}V_2$ was recorded at several temperatures between 107 and 157 K, a temperature interval over which the hyperfine lines begin to broaden (see Figure 7). The rate constant for intramolecular electron exchange at these temperatures is easily shown[40] to be

$$k = (3)^{1/2}\pi(g\beta/h)\Delta H_e \ s^{-1}$$

where ΔH_e is the contribution to the ESR line width from the exchange process. Overall line widths at temperatures between 107 and 157 K were found (by simulation of the experimental spectra) to vary from 30.0 to 35.6 G. Values of ΔH_e were obtained by subtracting an estimate of the line width under conditions of no exchange, ΔH_0. The latter value is uncertain but should lie between 10 G (the value for $P_2W_{17}V^{IV}$) and ~30 G (the value for $P_2W_{15}V^{IV}V_2$ at 77 K). We have therefore calculated sets of k's assuming ΔH_0 = 10, 15, 20, and 25 G. Each of these sets gives an acceptable Arrhenius plot (log k vs. T^{-1}) from the slopes of which E_a is found to lie between 140 and 500 cal mol^{-1} (0.006 and 0.022 eV). These values are to be contrasted with E_{th} calculated from the optical spectra (Table VII).

The values of k_{et} and J determined from the intervalence bands are consistent with the ESR results; the electron-transfer rates are "fast" on the ESR time scale, and superhyperfine structure was observed at low temperature. However, it is necessary to comment on the values in Table VII for $P_2W_{15}V_3$ which have been based on the absorption band at 13 700 cm^{-1}. The assignment of this band as the IT transition is by no means certain. The poorly defined weak shoulder at ca. 9000 cm^{-1} (see Table IV) is an alternative candidate, from which J = ~0.04 eV, E_{th} = ~0.24 eV, and k_{et} = ~1×10^{10} s^{-1} may be extracted. It is of interest to note that both spectral assignments lead to a larger value of E_{th} for $P_2W_{15}V_2$ than for the binuclear cases $P_2W_{16}V_2$ and $HP_2W_{15}V_3$. This result has recently been predicted. Launay and Babonneau[41] have described a "semiclassical" model for a trinuclear mixed-valence system. For such a system in which the in-phase combination of metal orbitals is the least stable, as is the case here with oxo-bridged metal atoms, the model predicts a greater energy barrier (E_{th}) than for a binuclear system with comparable dimensions and delocalization parameters.

The values of J in Table VII are smaller than those recently reported for some polymolybdates (0.15–0.34 eV),[42] a result which can be attributed both to the smaller extension of the 3d vs. 4d orbitals and to differences in bridging bond angles (edge- vs. corner-sharing of MO_6 octahedra).[43] The small values of J also account for the fact that the predicted splitting (by ~2 J) of the intervalence band in the trinuclear case could not be resolved.

Acknowledgment. We thank Dr. Hideo Kon (NIAMD, Bethesda, MD) and Dr. George Yang (FDA, Washington, DC) for the use of ESR spectrometers and variable-temperature accessories and for advice. Professor C. F. Hammer was also generous with time and assistance for the NMR spectroscopy. The research has been supported by NSF through Grant No. CHE-8019039.

Appendix

Separation of Isomers of $[P_2W_{17}VO_{62}]^{8-}$. About 30 g of Sephadex G50 (fine) was treated with 300 mL of dimethylformamide at 85 °C for 4 h. The gel was separated and soaked overnight in a 1:1 mixture of dimethylformamide and aqueous 0.5 M sodium acetate buffer, pH 4.7 (DBM). A 45 × 3.5 cm column was packed with the treated gel and rinsed with 250 mL of DBM. A solution of ca. 100 mg of the isomer mixture in 10 mL of DBM was placed on the column and eluted with DBM. The α_2-isomer is eluted before α_1. The same method has been used to separate β_1-, β_2- and β_3-isomers[44] of $[SiW_{11}VO_{40}]^{6-}$ and to separate mixtures of $P_2W_{15}V_3$ and $P_2W_{16}V_2$.

Registry No. P_2W_7V, 85585-36-0; $P_2W_{15}V_3$, 85585-42-8; $P_2W_{16}V_2$, 85585-37-1; $P_2W_{17}V^{IV}$, 12412-90-7; $P_2W_{16}V_2^{IV}$, 85585-39-3; $P_2W_{16}V^{IV}V^{V}$, 83333-29-3; $P_2W_{15}V_3^{IV}$, 85585-41-7; $P_2W_{15}V^{IV}V_2^{V}$, 83363-67-1; $[P_2W_{17}VO_{62}]^{7-}$, 85585-35-9; $[P_2W_{16}V_2O_{62}]^{8-}$, 85585-38-2; $[P_2W_{15}V_3O_{62}]^{9-}$, 85585-40-6; $K_{10}P_2W_{17}O_{61}$, 59111-46-5; $LiK_9P_2W_{17}O_{61}$, 63950-56-1; $VOSO_4$, 27774-13-6.

(36) Tetra-*n*-butylammonium salts of the heteropolyanions, soluble in these solvents, were obtained by shaking aqueous solutions with a benzene solution of Bu_4NCl. The benzene layer was separated and the solute recovered by allowing the solvent to evaporate at room temperature.

(37) Barcza, L.; Pope, M. T. *J. Phys. Chem.* **1975**, *79*, 92.
(38) Meyer, T. J. *Chem. Phys. Lett.* **1979**, *64*, 417.
(39) Brunschwig, B. S.; Logan, J.; Newton, M. D.; Sutin, N. *J. Am. Chem. Soc.* **1980**, *102*, 5798.
(40) Ward, R. L.; Weissman, S. I. *J. Am. Chem. Soc.* **1957**, *79*, 2086.
(41) Launay, J. P.; Babonneau, F. *Chem. Phys.* **1982**, *67*, 295.
(42) Sanchez, C.; Livage, J.; Launay, J. P.; Fournier, M.; Jeannin, Y. *J. Am. Chem. Soc.* **1982**, *104*, 3194.
(43) See part 2, in preparation.
(44) Sanchez, C.; Michaud, M.; Livage, J.; Hervé, G., *J. Inorg. Nucle. Chem.* **1981**, *43*, 2795.